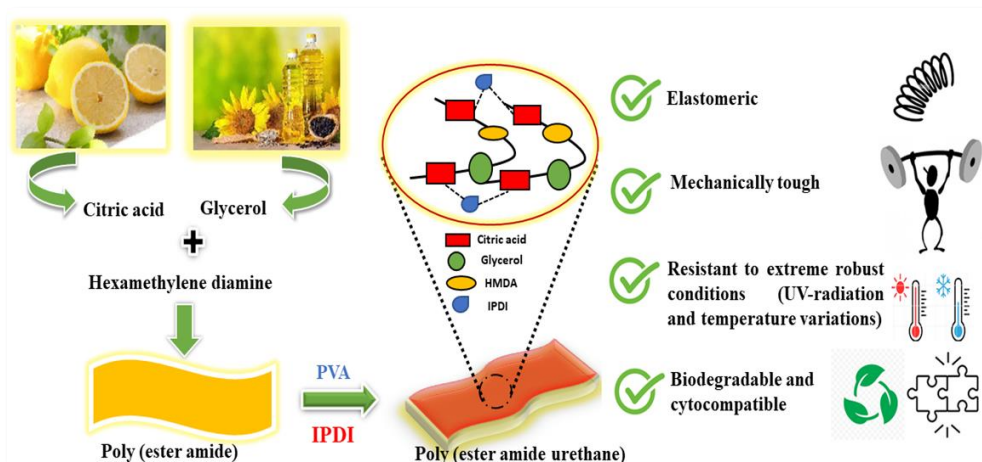


Chapter 3



Modification of poly(ester amide) to produce an elastomeric biodegradable poly(ester amide urethane) as a tough, robust, and biocompatible material

Highlights

Poly(ester amide)s belong to a special class of polymers and their intrinsic properties can be tailored by tuning their chemical structures. In this regard, poly(ester amide urethane) resins were prepared by modifying the poly(ester amide) to circumvent the shortcomings as well as to impart new features into the poly(ester amide) framework. In this chapter, various compositions of poly(ester amide urethane) were prepared by varying the proportions of isophorone diisocyanate. The structural analysis of the synthesized polymeric material was accomplished using various instrumental techniques viz., FTIR, XPS, PXRD, etc. On investigating the mechanical profile, it was noted that the polymeric specimens exhibited excellent elongation at break values ranging from 640.81% to 1875.91%, thereby rendering traits of a sturdy elastomeric material. The samples also demonstrated outstanding toughness values from 11.25.11 MJm⁻³ to 18.95.62 MJm⁻³. In turn, the polymeric material displayed satisfactory thermal stability, above 200 °C along with good chemical resistance values. Disparate aging tests were conducted to assess the durability of the material under stringent environmental conditions. The materials demonstrated remarkable enhancement in tensile strength parameters upon exposure to various aging regimes (heat, UV, etc.) which further promote their utility as robust materials for outdoor applications. Additionally, they revealed exceptionally good biodegradable attributes along with significant cytocompatibility behavior.

Parts of this chapter are published as

Kar, A., Rather M. A., Mandal, M., and Karak, N. Elastomeric biodegradable poly (ester amide urethane) as a tough and robust material. *Progress in Organic Coatings*, 182:107684, 2023.

3.1. Introduction

Chapter 1 enumerated the fact that over recent times, there has been a steep rise in the usage of synthetic polymers across the globe owing to the rapid rate of advancement in science and technology [1]. Synthetic polymers belong to a versatile category of polymeric materials and are known to cater the diversified demands of society ranging from textile industries, construction industries, paints, packaging sectors, etc. to pathbreaking scientific developments and innovations [2-4]. Nonetheless, keeping the benefits aside, the cause of utmost concern rests on the ground that these conventional man-made polymers are acquired from petroleum-derived feedstocks which are exhaustible in the long-time frame. Despite their ease of availability in nature and facile handling, they are triggering ultimatum to environmental well-being and sustainability. Moreover, it has become a pressing priority to focus as well as promote the usage of bio-derived polymers which are also sought to be biodegradable in nature taking into consideration the rising ecological awareness amidst common people [5-7]. In turn, the generation of such environmentally viable materials can aid in addressing as well as reducing harmful environmental consequences, viz., tons of litter generation from sturdy plastic materials and their disposal upon usage, release of potent greenhouse gases upon degradation, etc. [8]

Under this framework, poly(ester amide)s are regarded as a favorable class of polymers and are known to contain significant applicability in various segments as demonstrated extensively in **Chapter 1** [9]. Additionally, on account of their multifaceted nature, they are of predominant relevance to research analysts across the globe. The presence of ester and amide linkages in an interwove fashion in the same polymeric backbone renders coupling of the desirable attributes of both polyesters as well as polyamides [10-12]. Biodegradability factor is conferred on the polymeric entity on account of the presence of ester moieties, whereas the existence of the amide group attributes to superior mechanical and thermal features owing to its double bond characteristic along with the occurrence of strong hydrogen bonding interplay [13]. These days waterborne polymeric systems are gaining prominence over solvent driven ones on context of their favorable traits such as hassle free clean up, low level of odor amount, no release of noxious chemicals, etc. [14] The existence of various chemical entities viz., carboxylate, hydroxyl, etc. on the periphery of the polymeric framework help in bestowing water solubility attribute via carrying out interactions with the water molecules. Such systems are considered as prospective

sustainable materials in bioengineering as well as pharmaceutical domains as discussed in details in **Chapter 2** [15-17].

Gauging the aforementioned picture, it becomes befitting on our part to fabricate a material that can withstand stringent environmental conditions, i.e., various chemical media, ultraviolet radiation, temperature, etc. [18] Previous reports on synthesis of poly(ester amide) thermosets provided reasonable biodegradability aspect and high water solubility. However, the overall texture as well as the chemical resistance and mechanical profile results of these polymeric films were not satisfactory as studied in **Chapter 2**. To circumvent the shortcomings, urethane linkages were introduced into the parent polymeric matrix to toughen up the polymeric material for better performance.

Over the course of past few years, polyurethanes have occupied an important position in our day-to-day life on account of their usage in various domains in the form of coatings, insulation, rigid foams, flexible foams, elastomers, thermoplastics, etc. [19] They are regarded as one of the most versatile categories of polymers and are extensively explored due to their facile synthetic approaches under ambient reaction conditions or even under room temperature and tunable properties [20]. A range of various traits can be rendered to this explicit class of polymer by carrying out different modifications in the structure of the reacting moieties, viz., diisocyanate and polyol including both macroglycol and chain extender. Moreover, polyurethanes are known to exhibit manifold applications in diverse genres, viz., biomedical, electronics, automobile, packaging industries, construction, footwear, etc. [21] Despite their utilities in different fields, certain pragmatic issues such as high flammability rate, non-biodegradability, etc. impede their wide spread usage in a mass scale [22].

Therefore, in this present study, an attempt has been made to generate a biodegradable poly(ester amide urethane) bearing elastomeric properties. Herein, the parent poly(ester amide) was prepared applying an environmentally sound technique without consumption of any solvent and the obtained resin was found to be water soluble in nature [23]. In addition, poly(vinyl alcohol) (PVA) was introduced further to improvise the texture of the synthesized resin. Isophorone diisocyanate (IPDI) was used primarily as a curing agent in order to incorporate the urethane linkages and various compositions of resin/PVA/IPDI were synthesized. The polymeric material obtained was evaluated further and various tests

were conducted in order to incorporate some desirable properties which would turn out to be useful for carrying out applications in various realms including surface coatings.

3.2. Experimental

3.2.1. Materials

A variety of chemicals, including glycerol anhydrous, citric acid anhydrous, hexamethylene diamine, zinc chloride, potassium hydroxide (KOH), tartaric acid, PVA, oxalic acid, sodium hydroxide (NaOH), *para*-toluene sulfonic acid (*p*-TSA), sodium chloride (NaCl), hydrochloric acid (HCl) and ethanol (EtOH) were utilized. The specifications for these chemicals were consistent with those discussed in **Chapter 2** elaborately. Both the bacterial strains, viz., *Pseudomonas aeruginosa* and *Bacillus subtilis* were used for conducting the biodegradation study as indicated in **Chapter 2**.

IPDI was procured from Sigma Aldrich, USA. It is a highly reactive chemical compound, present in its liquid state at room temperature with a characteristic odor. It bears a molecular weight of 222.3 g/mol with high purity, often exceeding 98% along with a density value of 1.09 g/cm³. It has a boiling point of around 168-170 °C along with a melting point typically below -20 °C.

Dimethyl sulfoxide (DMSO) was obtained from Merck, India. It is a clear, colorless liquid with a density value of 1.10 g/cm³. It bears a molecular weight of 78.13 g/mol along with purity levels ranging from 99.5% to 99.9%. It has a boiling point of approximately 189 °C along with a melting point of approximately 18.4 °C. It was used in minute quantity to ensure facile mixing of the poly(ester amide urethane) resin.

Tetrahydrofuran (THF) was acquired from Merck, India. It is a clear, colorless liquid bearing a characteristic odor with a density value of 0.89 g/cm³. It bears a molecular weight of 72.11 g/mol along with purity values of 99%. It has a boiling point of approximately 66 °C and a melting point of approximately -108.5 °C. It was utilized in conducting the chemical aging test of the polymeric materials.

Hexane was obtained from Merck, India. It is a clear, colorless liquid with purity levels often exceeding 95% - 99%. It bears a molecular weight of 86.18 g/mol along with a

density value of 0.660 g/cm³. It has a boiling point of approximately 68.7 °C and a melting point of approximately -95 °C. It was utilized in carrying out the chemical aging test of polymeric materials.

3.2.2. Methods

3.2.2.1. Preparation of poly(ester amide) resin

Melt polycondensation route was employed to conduct the preparation of the parent poly(ester amide) resin between the key components, viz. citric acid, glycerol as well as hexamethylenediamine, as discussed extensively in **Chapter 2**. Briefly, the requisite amounts of the reactants were added based on the calculation of the total functionalities displayed by each reactive functional group of the reactants. Since there was formation of a neutral polymeric material, it was assumed that $f(-\text{COOH}) = f(-\text{OH}) + f(-\text{NH}_2)$; wherein f stands for possible reactive functionality. This was followed by heating up the reaction mixture at 140 °C continuously for 3 h under a vacuum environment. The end product was finally collected as a thick solid conglomerate before reaching the point of gelation. The acid value was constantly monitored throughout the reaction, in order to inspect the completion of it.

3.2.2.2. Synthesis of poly(ester amide urethane)

In order to ameliorate the texture as well as provide strength to the polymeric films formed, PVA was incorporated into the parent poly(ester amide) resin. Two different sets of polymeric blends were prepared by using two solvents, viz. water and DMSO. Both were introduced in nominal proportion conducive enough to assist the process of dissolution in an effective manner. Furthermore, the reaction blend was favored to heat constantly at 80 °C for 1 h prior to attainment of a consistent concoction.

In turn, for formation of poly(ester amide urethane), IPDI was introduced into the reaction blend. Different loadings of IPDI were eventually added slowly in a drop-wise pattern with the aid of a syringe into the reaction medium. Meanwhile, the reaction was allowed to run for about 30 minutes at 60 °C under the aforementioned reaction conditions until complete consumption of isocyanate was achieved. Every batch size of the reaction resulted in synthesis of around 8 grams of polymeric material.

Five different compositions were synthesized by altering the weight percentages of IPDI content in two diverse solvents viz. water and DMSO. For brevity, they were labeled correspondingly as PEAW 0%, PEAW 5%, PEAW 10%, PEAW 15% and PEAW 20% in water as well as PEAD 0%, PEAD 5%, PEAD 10%, PEAD 15% and PEAD 20% in DMSO as given in **Table 3.1**.

Table 3.1. Compositions of poly(ester amide) resin, PVA and IPDI.

Sample code	Poly(ester amide) resin (g)	PVA (g)	IPDI (g)
PEAW/D 0%	1	0.6	-
PEAW/D 5%	1	0.6	0.08
PEAW/D 10%	1	0.6	0.1
PEAW/D 15%	1	0.6	0.2
PEAW/D 20%	1	0.6	0.3

The polymeric contents present in two different solvents were eventually transferred to Teflon sheets and were dried in a hot-air oven for a time period of 5-7 days at 65 °C until they gained their touch-free state. Subsequently, the dried polymeric films were taken out and utilized for carrying out various analyses. All the polymeric films were finally cut into rectangular shapes bearing overall dimensions 60 × 10 mm² in order to conduct different tests. Moreover, all the tests were performed in triplicate.

3.2.3. Characterization

3.2.3.1. Structural analysis

The synthesized poly(ester amide urethane) and its various compositions bearing different loadings of IPDI underwent comprehensive characterization using various spectroscopic and analytical techniques inclusive of FTIR spectroscopy, X-ray photoelectron spectroscopy (XPS), CHN analysis and powder X-ray diffraction (PXRD). The details of

instrumentation for FTIR spectroscopy and CHN analyzer have already been elaborately discussed in **Chapter 2**. In turn, XPS study was carried out in a Thermo-Scientific XP spectrometer bearing the model number (ESCALAB 220 XL) involving 40 eV as well as 100 eV as constant analyzer energies for carrying out high resolution and survey spectra, respectively. Additionally, the PXRD (Bruker AXS, D8 focus, Germany) was used to study the diffraction patterns and to evaluate the crystallinity index. All other instrumentation and methodologies utilized to evaluate the performance characteristics, viz., mechanical, thermal, chemical resistance and biodegradation were meticulously discussed in **Chapter 2**.

3.2.3.2. Aging tests

With a view to assess the durability of the prepared polymeric samples against exposure to diverse environmental conditions, numerous aging tests have been specifically carried forward. Different aging regimes, viz. thermal, UV, chemical and solvent have been performed on both sets of polymeric blends and their mechanical as well as weight loss profiles were critically determined and analyzed for further applications.

3.2.3.2.1. Chemical aging

To conduct the above-mentioned test, polymeric specimens were cut in rectangular shape bearing overall dimensions $60 \times 10 \text{ mm}^2$. Three polymeric samples from each composition were taken into consideration for carrying out this aging procedure. The testing samples were placed in three different media possessing variable pH parameters, viz. acidic media (pH = 4-5), neutral media (pH = 7) and basic media (pH = 9-10) for a time period of 30 days at room temperature. After completion of the specified time period, the samples were removed from the media solution and were fully dried at room temperature for a time span of 48 h. Weight loss profiles of these specimens were further investigated in detail.

3.2.3.2.2. UV aging

In order to carry forward this test, polymeric samples (cut in rectangular size having dimension $60 \times 10 \text{ mm}^2$) were put under an UV light accelerated test chamber (UV aging chamber name- Almicro UV accelerated inspection cabinet, manufacturer - Micro measures & instruments, city and country - Ambala, Haryana, India, irradiation source -

fluorescent UV lamps, UV wavelength of source - 254 nm-365 nm, temperature - ambient room temperature $\sim 30\text{-}35\text{ }^{\circ}\text{C}$, relative humidity - $\geq 90\% \pm 5\%$, irradiation range - $0.4\text{-}1.4\text{ W/m}^2$, power supply - 380 V, 50 Hz). The UV-aging procedure was performed for a total time period of 150 h and a constant distance of 25 cm was precisely maintained between the UV source lamp and the polymeric specimens. After accomplishment of the requisite time period, the specimens were placed in a desiccator for 48 h at room temperature. Subsequently, their mechanical properties were analyzed and noted down to perceive the degree of aging underwent by the specimens.

3.2.3.2.3. Heat aging

Under this test, the polymeric samples were consigned to an artificial temperature controlling setup for a time span of seven days (approximately 170 h) at prescribed high and low temperatures, i.e., $70 \pm 2\text{ }^{\circ}\text{C}$ (Device - Convection oven, model name - NDO-710, manufacturer - EYELA World, city and country - Tokyo, Japan, power - 2 kW, power supply- single-phase, 110/220V $\pm 10\%$, 50/60 Hz) and $2 \pm 1\text{ }^{\circ}\text{C}$ (Device - Refrigerator, model name - RT28A3453BX/HL/2022, manufacturer - Samsung, city and country - Seoul, South Korea) respectively. Both high and low temperature zones were chosen to evaluate the durability of the prepared polymeric films. After completion of the experiment, the polymeric specimens were kept at room temperature for a period of 48 h and eventually mechanical features were assayed to study the extent of aging process.

3.2.3.2.4. Solvent aging

To conduct this test, polymeric samples of various compositions were immersed in three different solvents, i.e., ethanol, THF and hexane for a time span of 7 days. The films were gradually removed from the solvent media after completion of the specified time slot and the weight loss differences in percentage were further computed to note down the significant weight loss amount after the aging procedures.

3.2.3.3. Soil burial study

To carry out evaluation of the polymeric specimens under adverse natural conditions mimicking real field scenario, elemental analysis was primarily carried out to assess the soil composition using a CHN analyzer. Eventually, the pH of the soil was determined and

noted. In turn, the collected soil was properly sieved using a stainless-steel sieve and the unwanted pebbles, gravel and foreign matter were segregated. The polymeric samples bearing various compositions were weighed properly and placed inside paper cups filled up with collected specimen soil. The samples were buried deep in the soil bed at 10-12 cm depth and water was added regularly to maintain the overall moisture content of soil for a time period of 60 days. After completion of the specified time period, the samples were taken out carefully and washed properly with distilled water to get rid of unwanted foreign particles clung to the surface. Furthermore, the specimens were dried in hot air oven at 50 °C until a constant weight was obtained. The weight loss (%) parameter was evaluated using the following equation.

$$\text{Weight loss (\%)} = \frac{W_i - W_f}{W_i} \times 100 \quad (3.1)$$

where W_i and W_f are the initial and final weights of the polymeric specimen before and after the soil burial test.

3.2.3.4. Cytotoxicity study

In order to carry out this extensive study, kidney cells of human embryo (HEK 293) were grown exclusively in Dulbecco's Modified Eagle's Medium (DMEM) enriched further with 1% penicillin-streptomycin solution, 10% fetal bovine serum (FBS), 1% non-essential amino acid, 0.05% L-glutamine and 0.6% 4-(2-hydroxyethyl)-1-piperazineethanesulfonic acid (HEPES). In order to evaluate the cytotoxicity parameter of prepared polymeric specimen, 1×10^4 HEK 293 cells were cultured via a well-plate method comprising of 96-well plates at a specified temperature of 37 °C as well as 5% CO₂ (humidified atmosphere) for a regime of 24 h. Three various concentrations, viz. 62.5 $\mu\text{g mL}^{-1}$, 125 $\mu\text{g mL}^{-1}$ and 250 $\mu\text{g mL}^{-1}$ of the sterilized polymeric sample were seeded in the wells in the form of small discs. After 24 h of incubation, the cells were assessed in an inverted microscope (Zeiss, Model no. AXIOVERT A1) in order to analyze the cell viability as well as the cell morphology parameter. They were further treated with sterilized MTT reagent solution in a Galaxy 170 incubator used for cell culturing purpose at humidified atmosphere, i.e., 37 °C and 5% CO₂ for a time period of 4 h. MTT reagent got reduced to formazan (dark purple insoluble compound) on exposure to metabolically active cells possessing dehydrogenases of mitochondrial units. Furthermore, the formazan

crystals were allowed to dissolve in denaturing buffer solution (HCl, isopropanol and sodium dodecyl sulfate (SDS) and the absorbances were recorded eventually in the Thermo Scientific Multiskan GO microplate reader unit at 570 nm wavelength. Cell viability parameter was evaluated using the following expression as shown in equation (3.2) taking into account the production of formazan crystals in treated as well as untreated well plates.

$$\text{Cell viability (\%)} = \frac{\text{absorbance of sample}}{\text{absorbance of control sample}} \times 100 \quad (3.2)$$

3.3. Results and discussion

3.3.1. Preparation of poly(ester amide) resin

Chiefly, preparation of the parent poly(ester amide) resin was carried forth via a polycondensation route between the key reactants, viz. citric acid, glycerol and hexamethylenediamine as discussed in **Chapter 2**. One pot synthesis underlined minimum usage of chemicals, efficient time management as well as simplified chemical procedures for carrying out mass scale production for industrial purposes. The presence of various chemical groups on the edge of the polymeric network resulted in different interactions leading to the formation of chemical linkages such as ester and amide bond formations coupled with release of small molecules such as water molecules primarily known as condensates. Based on the reactivity profile displayed by the characteristic functional groups, there is selective formation of the requisite poly(ester amide) resin as the main product.

However, it was found that the resinous product so obtained was somewhat brittle in texture. In turn, it was also necessary to devise film building capacity in the resinous material to analyze various properties. In this milieu, PVA was introduced into the main polymeric matrix to fortify the overall polymeric material. Extensive hydrogen bonding interactions between the hydroxyl groups of PVA moieties and free carboxylic acid entities further helped in reinforcing the polymeric material.

IPDI is a well-known compound belonging to a category of aliphatic diisocyanates. It is widely utilized as a curing agent by building in urethane linkages in the base polymeric matrix. Herein, polyaddition reaction between the hydroxyl groups present on the

boundary of the polymeric framework and the isocyanate groups of IPDI results in formation of urethane linkages. Various spectroscopic studies were carried out in order to confirm the presence of urethane bonds in the polymer matrix. In turn, the plausible reaction scheme elucidating the steps required in formation of poly(ester amide urethane) i.e. initial fabrication step of preparation of poly(ester amide) resin followed by gelatinization step with PVA via hydrogen bonding interactions to final dropwise addition of IPDI is clearly shown in **Scheme 3.1**.

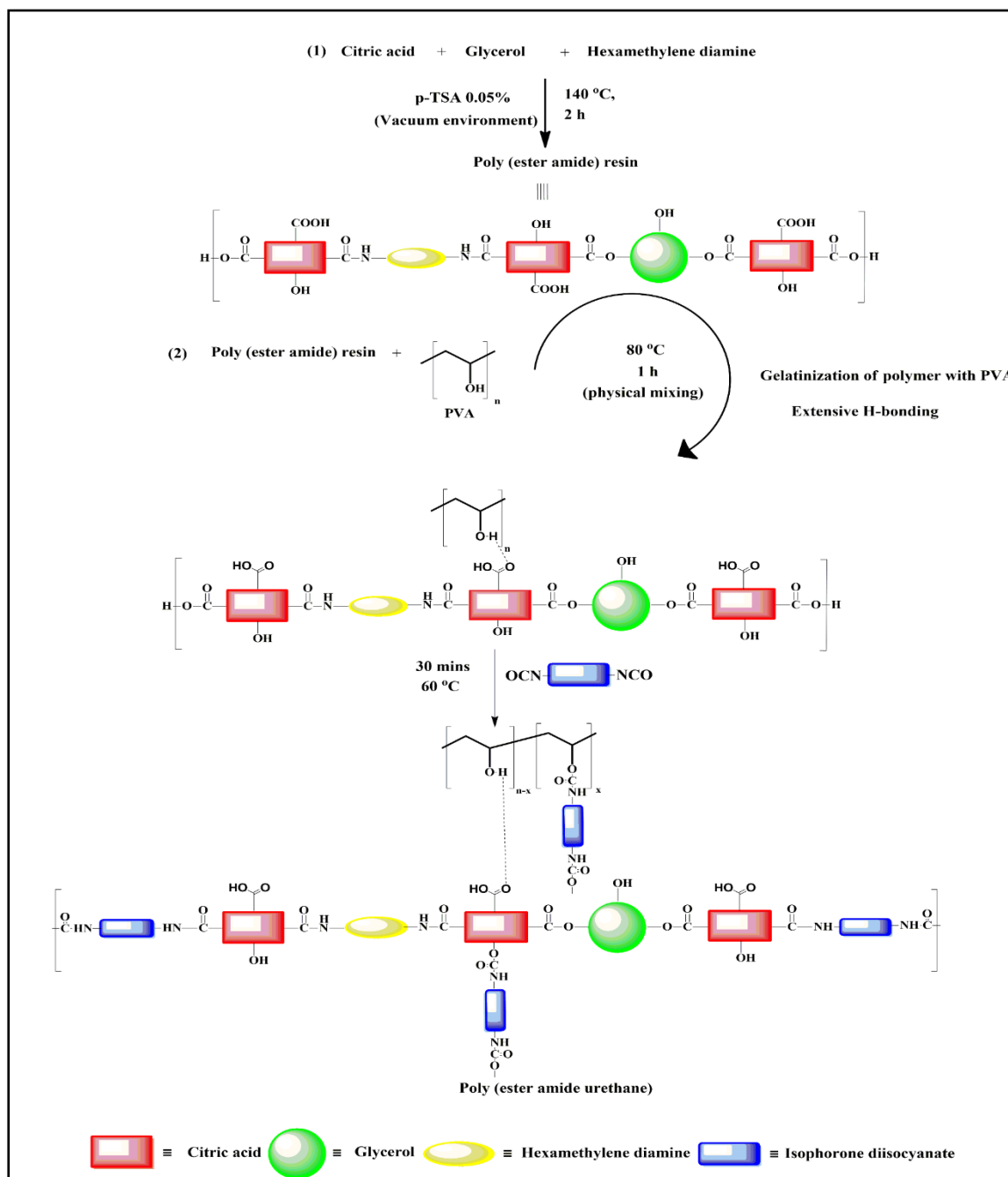
Both DMSO and water were used to assist facile formation of polymer blends. Water, being a benign solvent was utilized for casting the polymer blend unit; however, the texture of the polymeric films was found to be rough on account of formation of blisters due to release of carbon dioxide gas trapped beneath the surface of the films. Herein, carbon dioxide is formed in view of the reaction between isocyanate and water. So, in order to upgrade the texture quality of the films, DMSO was further used as the solvent casting medium. Both the solvents exhibited satisfactory compatibility with the polymeric material which paved the way for homogeneous mixing for formation of polymer blend. The properties of the polymeric material in both the solvents were further explored extensively as discussed later on.

3.3.2. Physical features

The parent poly(ester amide) resin was found to be brown in color wherein the poly(ester amide urethane) resin prepared in two different solvents of varying compositions exhibited different colors. Polymeric samples blended in DMSO solvent displayed dark brown color, whereas those dissolved in water exhibited light yellow brown color. In turn, specific gravity parameter was assessed using the standard liquid displacement method and the necessary calculations were carried out for all compositions in two different solvents, viz. water and DMSO as produced in **Table 3.2**.

It was keenly observed that with enhancement of IPDI concentration in the polymer framework, a linear increment was noted down in the density values. This is suggestive of the fact that increase in IPDI content, resulted in greater number of urethane linkages leading to intensified molecular interactions between polar groups. Consequently, a rigid

compact dense structure was formed which goes concurrently with the rise in density values.



Scheme 3.1. Plausible reaction scheme for synthesis of poly(ester amide urethane) resin.

3.3.3. Structural analysis

The confirmation of the poly(ester amide urethane) structure was carried out through

different spectral analyses which are inclusive of FTIR, XPS, PXRD, etc.

Table 3.2. Density of poly(ester amide urethane) resin at various compositions in two different solvents, DMSO and water.

Property	PEA 0%	PEA 5%	PEA 10%	PEA 15%	PEA 20%
Density at 25 °C (g cm ⁻³) DMSO	0.87	0.89	0.91	0.94	0.95
Water	0.91	0.93	0.95	0.96	0.99

3.3.3.1. FTIR spectral study

FTIR spectral analysis is carried out to inspect the presence of different functional groups within the polymeric matrix. The FTIR spectra displayed in **Figure 3.1.** typifies the existence of various chemical groups in the synthesized poly(ester amide) urethane resin. The broad absorption band observed at 3398 cm⁻¹ attributed to -OH stretching vibrations which verified the presence of hydroxyl groups in the polymer backbone. It is a well perceived fact that -OH and -NH bands tend to overlap with each other. Under this pretext, prominent peaks of -NH absorption bands are difficult to obtain in the spectra. Moreover, -OH bonds are considered to be more polar than -NH bonds on account of their differences in electronegativity values; so broad and intense absorption bands for -NH stretching vibrations are not available. Furthermore, IR spectral peaks at 2863 cm⁻¹ and 2952 cm⁻¹ ascribed to symmetric and asymmetric stretching vibrations of C-H units belonging to an aliphatic framework, respectively. In addition, the stretching vibrations for carbonyl group in amide and urethane units were observed at 1632 cm⁻¹ and 1734 cm⁻¹, respectively. The inset diagram incorporated in the FTIR spectra closely illustrated the carbonyl peak of urethane for the resin material and its various compositions. This further proclaimed the significant formation of amide and urethane linkages in the polymer material. Characteristic absorption bands at 1141 cm⁻¹ corresponded to -CN stretching vibrations, wherein spectral peaks at 1247 cm⁻¹ referred to -COC stretching vibrations. Furthermore, IR absorption frequency at 1072 cm⁻¹ elucidated -CO stretching vibration of ester moiety [24]. Therefore, FTIR spectral studies aided in successful investigation of chemical

structure of the poly(ester amide urethane) resin and its varied compositions.

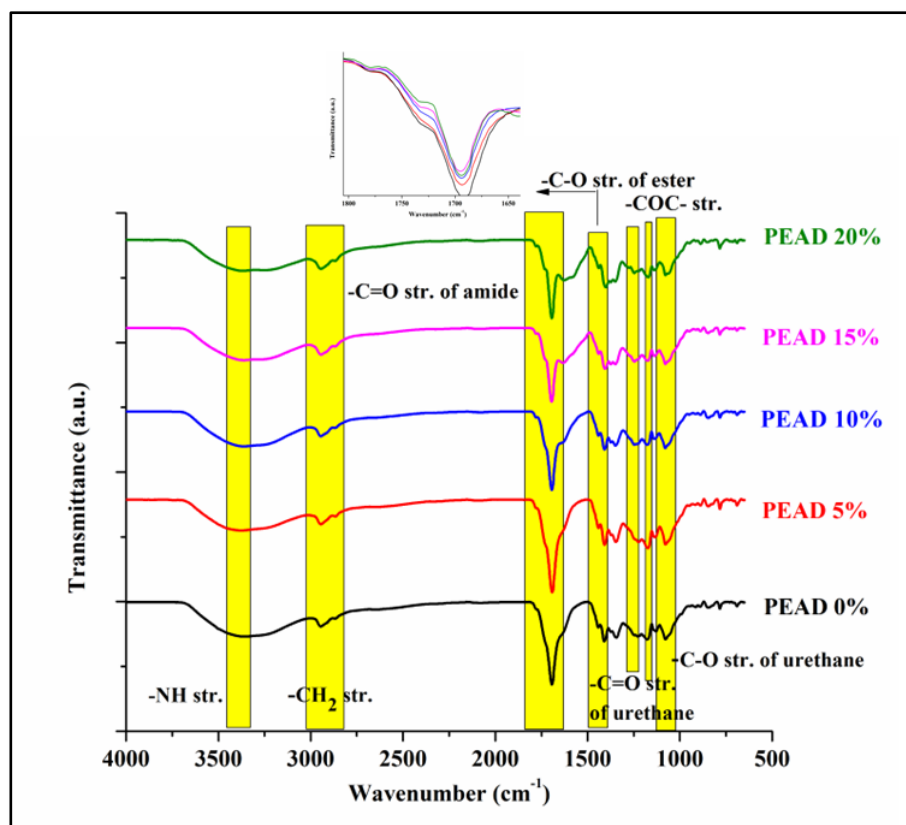


Figure 3.1. FTIR spectra of different poly(ester amide urethane) compositions with various loadings of IPDI.

3.3.3.2. XPS analysis

XPS study is carried out to analyze the surface composition of a polymeric specimen. Herein, XPS was exclusively used as an analytical tool to shed light on the chemical composition of poly(ester amide urethane) material as shown in **Figure 3.2**. Detailed investigation of the analysis revealed the presence of C, N, and O as the basic elements of polymer skeleton bearing atomic fractions of 60.91%, 6.69% and 32.41%, respectively. Moreover, thorough assessment was carried out by exploring the high resolution XPS spectra of C1s, N1s and O1s of poly(ester amide urethane) material [25]. Under this pretext, the C 1s peak is deconvoluted into three peaks, which are assigned specifically to C-H and C-C at 284.61 eV, C-N and C-O at 285.57 eV and C=O and O-C-O at 287 eV [**Figure 3.2. (b)**]. All these spectral peaks are evaluated as representative peaks of carbon containing entities viz., citric acid, glycerol, hexamethylenediamine, etc. Similarly, for O

1s XPS plot, the peak at 531.22 eV is attributed to C-O and C-O-C groups, wherein the peak at 532.63 is assigned to C=O functional group, respectively. The presence of citric acid moiety and the formation of C-O linkages amidst the monomeric units are confirmed by the deconvoluted O peaks of XPS spectra [Figure 3.2. (c)]. In turn, the N 1s spectrum is deconvoluted into two peaks at 399.78 eV and 402.28 eV which are accredited to N-H and N-C groups, respectively [Figure 3.2. (d)]. The deconvoluted N peaks established the presence of hexamethylenediamine and IPDI moieties in the framework.

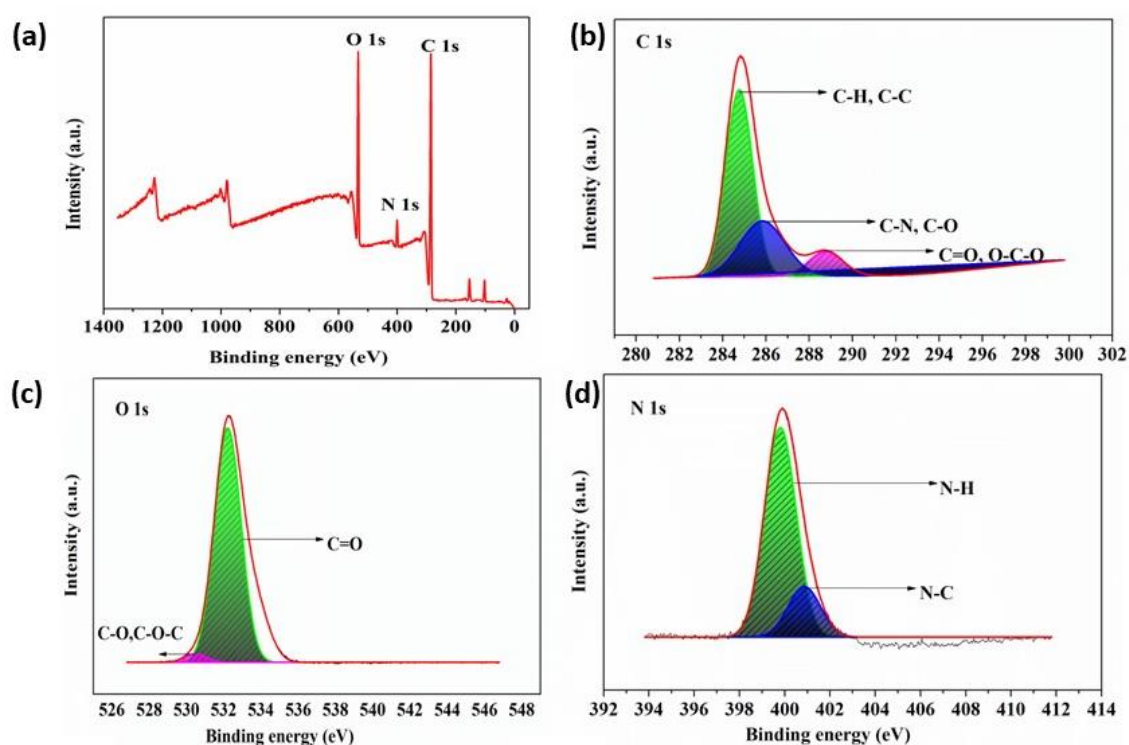


Figure 3.2. (a) XPS survey spectra, and deconvolution of (b) C 1s, (c) O 1s and (d) N 1s high-resolution spectra for poly(ester amide urethane) film.

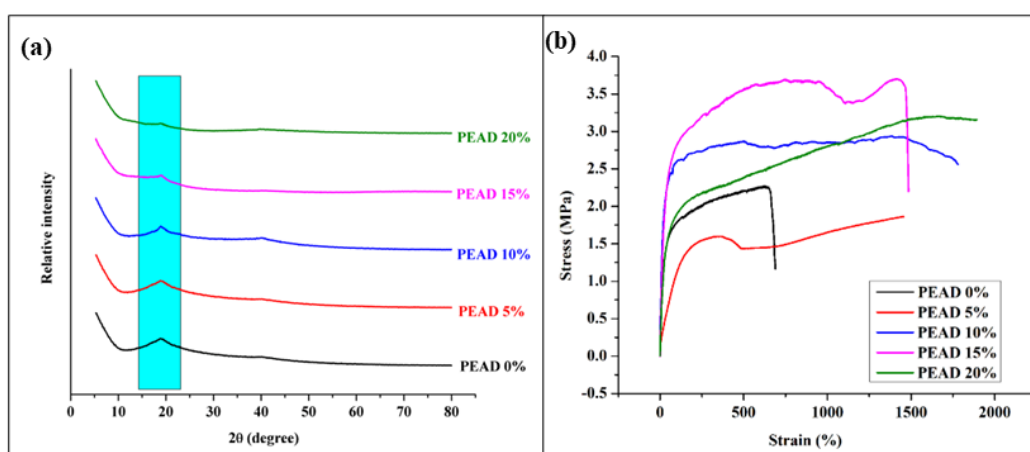
3.3.3.3. X-ray diffraction analysis

XRD study is considered as an effective parameter to characterize polymeric substances. Herein, PXRD was used extensively to assess the structural information of poly(ester amide urethane) and its films of varying compositions as depicted in Figure 3.3. (a). It is a well-noted fact that crystalline substances exhibit sharp, intense and well-defined peaks, wherein amorphous substances display relatively broader peaks in the XRD spectra. In this milieu, as per earlier literature reports, it is found that PVA exhibits a diffraction peak at

19.5° which is broad in nature and elucidates the amorphous feature of the material [26]. The XRD spectra obtained in **Figure 3.3. (a)** verified the presence of PVA in the polymer skeleton with its characteristic peak at $2\theta = 19.09^\circ$. In this study, PEAD 0% composition exhibited the highest intense peak, wherein PEAD 20% highlighted extensive broadening in peak with diminished intensity level. This could be suggestive of the fact that with increment in IPDI proportion, extensive interactions occurred between the hydroxyl groups of PVA moiety leading to loss in semi-crystalline properties of PVA. Thus, XRD studies provided satisfactory information about the amorphous nature of poly(ester amide urethane) resin and its different compositions.

3.3.4. Mechanical properties

Evaluation of the mechanical features viz., tensile strength, elongation at break, toughness, impact resistance and scratch hardness were carried out to invoke its utility and all the mechanical parameters were listed in a tabulated manner in **Table 3.3**. It was found that these traits depend largely on a variety of factors which are inclusive of the molecular weight of the entire polymer skeleton, different constituents of the framework and their types, existence of manifold inter and intra molecular forces of interaction, presence of extensive hydrogen bonding interactions, ubiquitous polar functional groups layered on the surface of polymeric material, degree of entanglement by polymeric chains, etc. [24,



27]

Figure 3.3. (a) XRD spectra and (b) stress-strain profiles of poly(ester amide urethane) with different compositions.

From the extensive mechanical assessment as depicted in **Figure 3.3 (b)**, it could be stated that the mechanical parameters varied significantly with the change in amount of IPDI. It was observed that adequate amount of crosslinking facilitated various forces of interaction to come into existence, thereby attributing to considerable amount of rigidity as well as providing a strained environment to the structure in totality. It was noted that increase in the content of IPDI resulted in greater tensile strength values. The reason behind this trend could be explained on the ground that IPDI, being an excellent crosslinker promoted substantial number of intermolecular interactions leading to greater tensile strength values with subsequent increment in its proportion. In turn, elongation at break values were also found to escalate with marked increase in the proportion of IPDI [28]. Apart from enhancing the crosslinking density of the polymeric framework by various intermolecular interactions, IPDI also acted as a bridge between two polymeric segments, thereby

Table 3.3. Mechanical features of poly(ester amide urethane) with various compositions.

Property	PEAD 0%	PEAD 5%	PEAD 10%	PEAD 15%	PEAD 20%
Tensile strength (MPa)	2.25 ± 0.015	1.84 ± 0.014	2.58 ± 0.015	3.68 ± 0.007	3.16 ± 0.012
Elongation at break (%)	640.81± 0.12	1439.96 ± 0.11	1777.38 ± 0.15	1431.37 ± 0.10	1875.91 ± 0.12
Toughness (MJm⁻³)	11.25 ± 0.2	14.59 ± 0.1	17.80 ± 0.1	14.84 ± 0.4	18.95 ± 0.4
Impact resistance (kJ/m²)	10.13 ± 0.3	10.49 ± 0.3	10.55 ± 0.5	13.97 ± 0.3	14.95 ± 0.5
Scratch hardness (kg)	5 ± 0.3	6 ± 0.3	6 ± 0.2	7.5 ± 0.3	7.5 ± 0.5
Gloss at 60°	90 ± 5	90 ± 6	92 ± 5	94 ± 5	94 ± 6

increasing the hydrocarbon content of the entire framework and making the entire system more flexible. In addition, release of the entangled chains along with rupture of the secondary forces of interaction resulted in causing the elongation parameter to rise up with further increment in the amount of crosslinker. In a similar way, the toughness values were calculated by carrying out integration under the stress-strain profile and they displayed a similar trend as discussed above. Additionally, it was found that the impact resistance and scratch hardness parameters exhibited a rise in its value with increment in the content of IPDI. The reason behind this pattern can be explained on the pretext that increase in amount of IPDI resulted in promoting perfect synergism between the elongation at break as well as tensile strength parameters. Likewise, the gloss parameters of the polymeric films also exhibited splendid results owing to the presence of a smooth surface as well as magnificent dimensional constancy. Additionally, polymeric specimens (PEA 15% composition) were also prepared in six different solvent media, viz., pure water solvent, pure DMSO solvent, 50% ethanol/water, 70% ethanol/water, 10% DMSO/water and 50% DMSO/water in order to assess their texture as well as mechanical parameters. A comparative assessment was carried out to chalk out the best solvent system.

Herein, digital photographs of each polymer system in different solvent are provided (**Figure 3.4.**) to assess the texture of the films. It can be stated that presence of water in each of these systems (except pure DMSO) resulted in formation of extensive blisters owing to the release of carbon dioxide gas trapped beneath the films due to the reaction between isocyanate and water. This resulted in coarse texture for all the polymeric films. Highest coarse textured was obtained for pure water system, wherein pure DMSO polymeric specimen exhibited the smooth textured surface.

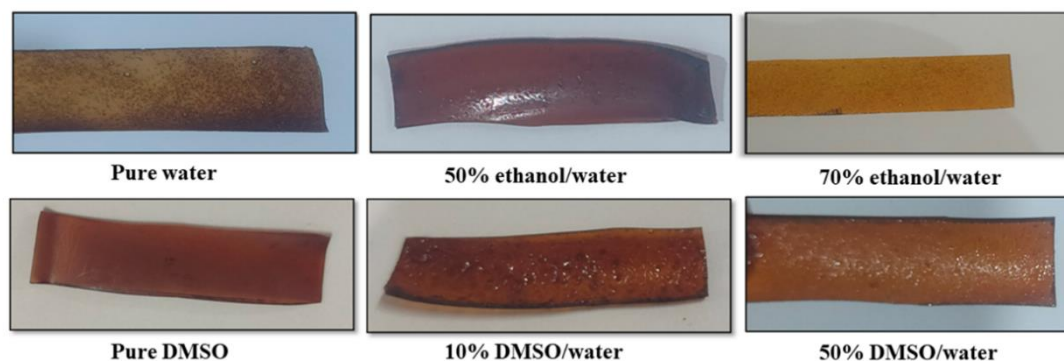


Figure 3.4. Digital photographs of poly(ester amide urethane) films (PEA 15% composition) in different solvents.

Evaluation of the mechanical properties, viz. tensile strength and elongation at break of poly(ester amide urethane) were also carried forward as depicted below in **Figure 3.5**. It could be stated that both these parameters varied significantly with change in the nature of solvents. Pure water polymeric system displayed tensile strength of around 4.5 MPa along with an elongation parameter of 720%; wherein 70% ethanol/water system showed a drastic dip in both tensile strength as well as elongation at break traits (2.5 MPa against 330%). In turn, the pure DMSO system exhibited tensile strength of around 3.4 MPa along with an elongation at break property of 1215%; on the other hand, 50% DMSO polymeric unit exhibited a significant drop in mechanical parameters (1.25 MPa against 1028%).

Therefore, it can be concluded that DMSO based polymeric system served as a better system taking into consideration the smooth texture as well as satisfactory mechanical traits of the polymeric specimens.

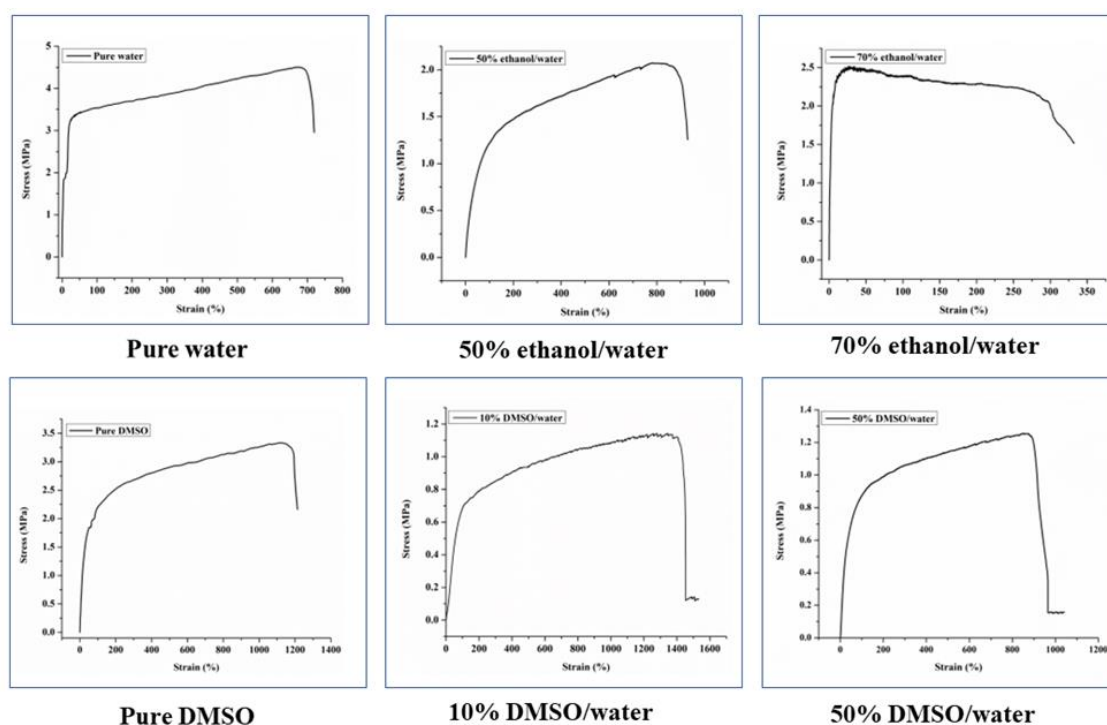


Figure 3.5. Stress-strain profiles of poly(ester amide urethane) films (PEA 15% composition) in different solvents.

3.3.5. Thermal properties

TGA and DSC analyses were carried out to evaluate the thermal traits of poly(ester amide

urethane) and its different compositions. A careful investigation of the thermal degradation curves of all the five compositions of poly(ester amide urethane) revealed the fact that all of them employed a two-step degradation profile as illustrated exclusively in **Figure 3.6**. In turn, all the other thermal degradation variables viz., degradation onset temperature (T_{on}), glass transition temperature (T_g) and degradation peak temperature at two steps are tabulated explicitly in **Table 3.4**. It was observed that the beginning of thermal degradation simply initiated off with the loss of small entities such as water molecules or other volatile moieties which were adsorbed on the surface of the polymeric network. In addition, the real thermal degradation started off in the temperature range 175-187 °C which ascribed to the breakage of aliphatic portions present in the polymeric skeleton as well as the ester linkages which are known to be labile in nature under thermal conditions. Moreover, the second degradation was spotted in the temperature range 382-475 °C which attributed to

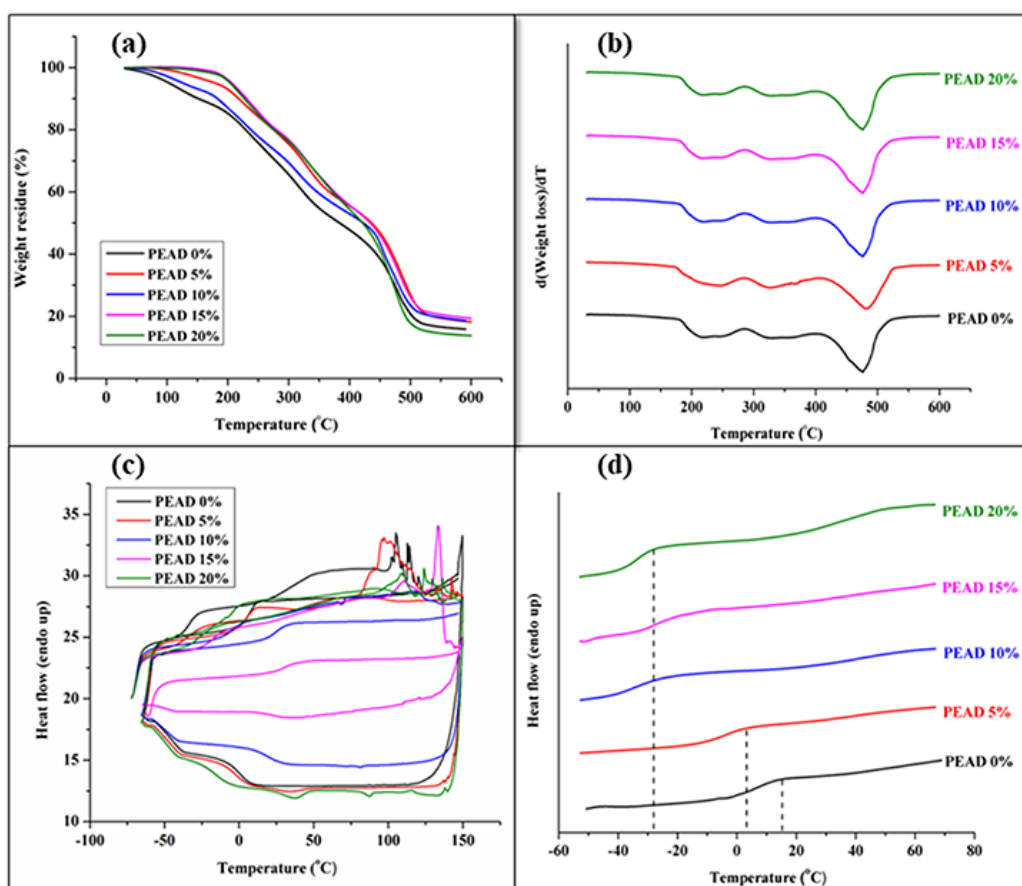


Figure 3.6. (a) TGA curves, (b) DTG curves, (c) DSC heating-cooling-heating curves and (d) DSC curves exhibiting T_g s of poly(ester amide urethane) with various compositions.

the rupture of thermally stable urethane and amide linkages along with the degeneration of PVA framework. The region after 475 °C was assigned to the generation of charred or carbonaceous end products of black carbon. Furthermore, the weight loss residues were assessed at 600 °C after conducting the thermal degradation study and they were found to be satisfactory. These data implied that these polymeric specimens remained thermally stable even under such high temperature [Figure 3.6. (a) and Figure 3.6. (b)].

DSC studies were also conducted to calculate the T_g value as revealed in Figure 3.6. (c) and 3.6. (d) which were observed to fall in the temperature range of 15 to -28 °C. Additionally, it was found out that the polymeric material bear only one soft segment which corresponded to only one T_g value for each polymeric composition as reported in Table 3.4. This reaffirmed the absence of any hard segment in the polymeric material. In turn, the endothermic peaks observed in the first heating curve of DSC study corresponded to the loss of moisture content absorbed by the polymeric films as illustrated in Figure 3.6. (c). It

Table 3.4. Thermal degradation variables for poly(ester amide urethane) with various compositions.

Variables	PEAD 0%	PEAD 5%	PEAD 10%	PEAD 15%	PEAD 20%
T_{on} (°C)	175	177	180	182	187
1st stage degradation peak temperature (°C)	224	225	228	231	236
2nd stage degradation peak temperature (°C)	475	477	478	480	482
Weight residue (%) at 600 °C	16	18	18.60	19.07	13.91
Glass transition temperature, T_g (°C)	15.16	3.26	-28.39	-28.15	-27.93

was also observed that the introduction of IPDI into the polymeric framework resulted in lowering the T_g value. This could be perceived on the ground that IPDI ensured amplifying the hydrocarbon content as well as facilitated increase in the free volume of the polymeric

surface. This caused the mesh network formation to glide against each other devoid of any obstacles with IPDI serving as a bridge between the polymeric fragments; ultimately leading to a sharp drop in the T_g value.

3.3.6. Chemical resistance

It is regarded as an essential feature to evaluate the chemical resistivity of poly(ester amide urethane) films under exposure to different chemical environments. The chemical resistance behavior was analyzed by conducting an extensive study on poly(ester amide urethane) film and its varied compositions for a time regime of 21 days under harsh chemical backdrop. The weight loss (%) profiles were subsequently calculated to evaluate their resistivity values in a comprehensive manner as documented in **Table 3.5**. It was observed that the poly(ester amide urethane) film and its compositions exhibited high resistance towards aqueous, saline (10% NaCl), alcoholic (10% EtOH) and acidic (5% HCl) media. On the other end, they showed relatively less resistance values towards alkaline chemical media (5% NaOH). This could be accounted on the ground that the ester as well as urethane linkages present in the polymer backbone are susceptible to hydrolysis under coarse alkaline environments. Additionally, existence of polar groups such as carboxylic, hydroxyl, etc. on the periphery of the polymeric framework resulted in establishing strong intermolecular forces of interaction leading to increased resistivity values against saline, alcoholic, acidic and aqueous media. In turn, it was also found that poly(ester amide urethane) demonstrated better defiance against chemical environments mentioned above in comparison to parent poly(ester amide) material. This could be cited on the pretext that poly(ester amide urethane) possessed greater level of urethane connectivity which attributed to better resistance values even under alkaline conditions.

3.3.7 Aging studies

These tests are conducted to evaluate the durability of a material under exposure to various stringent environmental conditions. All the polymeric samples were subject to various aging tests in order to establish their utility as prospective materials in various domains. In turn, assessments of their weight loss values and mechanical properties were evaluated to understand their robustness after post-aging treatments. The following sections gave a comprehensive analysis of all the aging tests along with their results in a detailed manner.

Table 3.5. Chemical resistance as weight loss (%) of poly(ester amide urethane) with different compositions.

Sample	5% NaOH	5% HCl	10% NaCl	10 % EtOH	Water
PEAD 0%	1.14	0.43	0.023	0.011	0.016
PEAD 5%	1.27	0.68	0.051	0.035	0.029
PEAD 10%	1.34	0.98	0.063	0.065	0.057
PEAD 15%	1.67	1.45	0.12	0.085	0.089
PEAD 20%	1.89	1.58	0.17	0.14	0.17

3.3.7.1 Heat aging

This aging test was conducted under two different temperature genres viz., 70 ± 2 °C and 2 ± 1 °C for a time period of 170 h followed by measurement of tensile strength values. As per earlier literature reports, it is noted that thermal exposure of polymeric samples results in either enhancement or restoration of tensile strength parameters owing to a variety of reasons such as increase in crosslinking density, crystallinity as well as reduction in mobility of polymer chains [29]. In this study, it was observed that there was improvement in the tensile strength values for all compositions of PEAD samples for both the temperature domains i.e., 70 °C as well as 2 °C as shown in **Figure 3.7. (a)** and **5(b)**. However, no such regular trend in the stress-strain profile was obtained. These deflections could be attributed to the physicochemical changes adopted by the samples under harsh temperature conditions. When the samples were subjected to elevated temperature, there was rise in crosslinking density owing to hike in tensile strength values and drop in elongation at break parameters, wherein the samples exposed at low temperature also exhibited rise in tensile strength variable due to increase in stiffness parameter on account of restricted movement of polymeric chains under low temperature. PEAD 15% showed a rise in tensile strength value from 3.68 MPa to 4.31 MPa and a drop in elongation at break value from 1431.37% to 1354%. This implied the fact that these specimens responded well to the thermal aging procedure. Therefore, these outcomes substantiated the merits of the synthesized specimen over other reported ones for temperature related applications.

3.3.7.2 UV aging

UV resistance displayed by the polymeric films is regarded as a vital parameter to assess the utility of the material for outdoor applications. As per literature sources, UV aging procedure works under a complex mechanism which exclusively includes rupture of the polymeric chains, rearrangement or remodeling of the molecular patterns, crosslinking, etc. which ultimately result in creating stiffness in the specimens [30]. In this investigation, all polymeric samples were subject to UV light exposure for a prolonged time period (150 h). It was found that all the compositions executed brilliant resistance against UV light exposure. This statement was supported by studying the stress-strain profiles of polymeric samples after undergoing aging procedures for the requisite time frame as shown in **Figure 3.7. (c)**. Although exposure to UV radiation results in breakage of chemical bonds due to photooxidation leading to decrease in tensile strength parameter but on the other hand, recombination of the polymeric chains leads to surge in the crosslinking density amount which further escalate the tensile strength parameter. In this study, recombination factor dominated the bond scission effect, resulting in enhancement of tensile strength values over earlier ones reported in this investigation. Therefore, these results favored the usage of these polymeric materials as UV resistant potent substances.

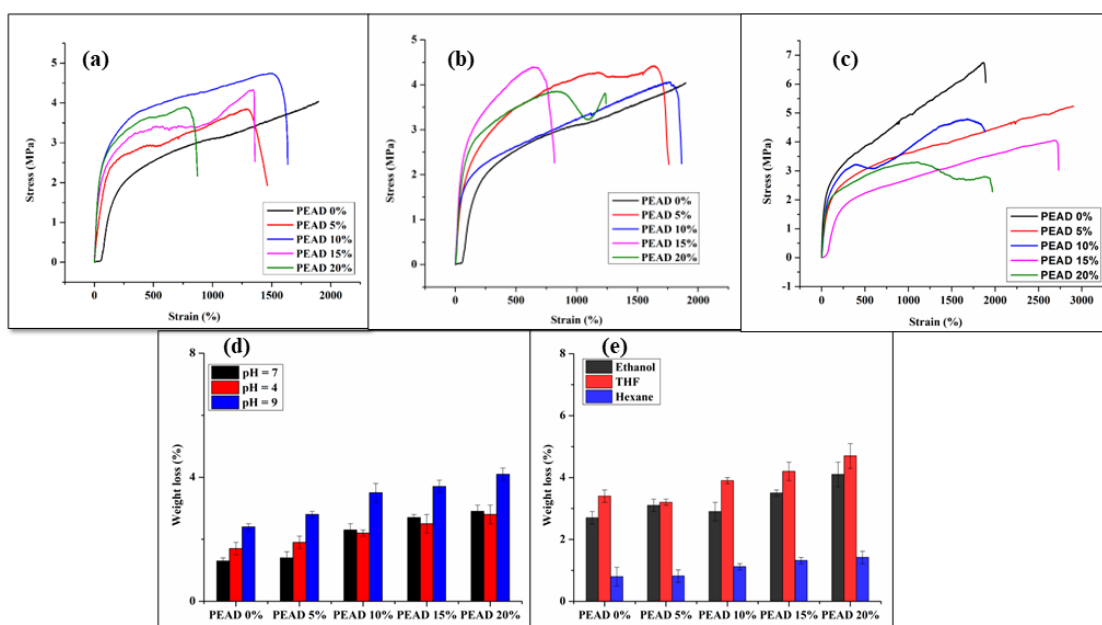


Figure 3.7. Stress strain profiles of poly(ester amide urethane) after (a) heat aging at 70 °C (b) heat aging at 2 °C (c) UV aging, and weight loss profiles after (d) chemical aging and (e) solvent aging.

3.3.7.3 Chemical aging

This aging procedure was carried out to inspect the robustness of the material under diverse chemical environments for a time period of 30 days. Weight loss assessment profiles as depicted in **Figure 3.7. (d)** highlighted the chemical resistance of all the compositions of PEAD under varying pH media. From the figure, it could be clearly stated that all the compositions executed satisfactory resistance towards acidic and neutral media, wherein very poor defiance was shown towards basic media. According to literature reports, diffusion of solution through the interstitial voids of polymer matrix is governed by Fick's law. Herein, the absorbed solution molecules of varying pH tend to occupy various crevices of the polymer framework; thereby carrying out disruption or fragmentation of the bonds via hydrolysis which result in weight loss [31]. The specimens exhibited significant amount of weight losses in alkaline media on ground of extensive alkaline hydrolysis of ester, amide as well as urethane linkages. Therefore, these artificially induced weathering conditions could test the durability of the specimens under critical conditions.

3.3.7.4 Solvent aging

This aging technique was conducted to analyze the resilience of the polymeric specimens under exposure to various solvents viz., ethanol, THF and hexane. All the samples were introduced in these solvents for a time frame of 7 days followed by computing their weight loss differences. As per literature sources, these solvent molecules eventually get entrapped inside the cavities of polymer framework, leading to deformations in their structure which gets reflected in the form of considerable amount of loss in the weight of the samples. Leaching can be cited to be one of the foremost reasons for surface degradation of these specimens, thereby triggering weight reduction in these specimens. In this present investigation, the highest weight loss was recorded for THF solvent, wherein the lowest weight loss was observed for hexane solvent as shown in **Figure 3.7. (e)**.

3.3.8 Biodegradation study

3.3.8.1 Microbial growth study

The biodegradability aspect of poly(ester amide urethane) film was scrutinized by conducting a microbial growth study against two different bacterial strains, viz. *Pseudomonas aeruginosa*, gram negative and *Bacillus subtilis*, gram positive bacteria for a time frame of 35 days. Both the strains are omnipresent in environment and aerobic in nature. **Figure 3.8.** (a) exposed the fact that the polymeric surface area got substantially degraded to a considerable extent which further implied that the polymeric base material served as a great source of catabolite [32]. The reason behind this extensive erosion could be cited on the ground that the poly(ester amide urethane) possessed ester as well as urethane linkages which are highly conducive to hydrolysis resulting in fragmentation of the polymeric specimen into smaller segments. In turn, addition of the poly(ester amide urethane) and its varied compositions into the culture media resulted in profound growth

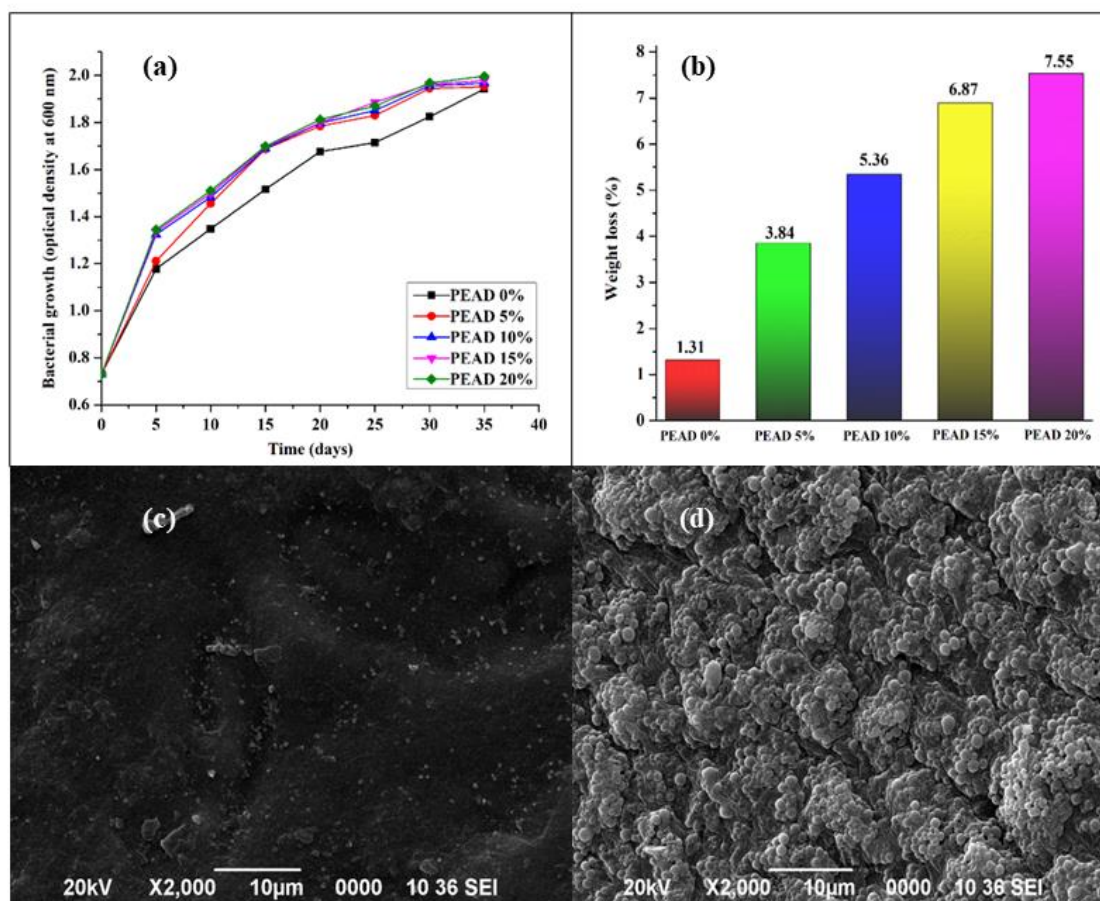


Figure 3.8. (a) Change in *Bacillus subtilis* growth, (b) weight loss (%) profile of poly(ester amide urethane) of all compositions against exposure time; SEM images of PEAD 15% composition (c) control specimen and (d) biodegraded by bacteria strain, *Bacillus subtilis*.

of bacteria which further led to rupture of urethane and ester connectivity into smaller fragments. These smaller molecules eventually diffuse into the basal media facilitating solubilization and further leading to formation of small units viz., water, carbon dioxide, etc. Furthermore, the weight loss profiles as shown in **Figure 3.8. (b)** are illustrative of the fact that the increment in proportion of IPDI resulted in greater rate of biodegradation. This interpreted the bottom-line fact that increase in number of urethane linkages ensured enhanced biodegradation rate with eventual addition of IPDI. The SEM images as depicted in **Figure 3.8. (c)** and **(d)** provided a clear-cut picture about the extent of biodegradation assay undergone by the polymeric specimen for a stint of 35 days. The comparison between the images of the control sample (bereft of polymer) and the degraded specimen clearly depicted the extensive rate of microbial degradation encountered by poly(ester amide urethane) and its diverse compositions.

3.3.8.2 Soil burial study

Another facet of biodegradability assay was evaluated by conducting the soil burial test. Herein, the samples were subject to real field circumstances under the intervention of soil bacteria. First and foremost, the chemical composition of the soil organic matter was analyzed using a CHN analyzer and the primary soil components were eventually determined (carbon: 5.32%, hydrogen: 0.6% and nitrogen: 0%). Moreover, the pH of the soil was ascertained to be moderately alkaline in nature (pH = 8.71). The extent of degradation as well as changes in surface morphology were studied by measuring the gravimetric weight loss profiles and carrying out SEM image studies [33, 34]. The figure as elucidated in **Figure 3.9. (a)** represented the weight loss (%) study of all the compositions of poly(ester amide urethane) for a time stretch of 50 days. It could be inferred from the bar graph that the material bearing the highest percentage of IPDI i.e., PEAD 20% displayed maximum weight loss (%) values. This could be substantiated on the ground that the polymeric specimen bearing the highest number of urethane linkages enabled extensive microbial attack on its surface since urethane bonds are subject to easy hydrolysis and thus prominent weight loss results are obtained. These results are in absolute agreement with previous literature reports which state that surface attack is the predominant mode of attack adopted by bacteria to carry out the degradation procedure which tend to considerable weight loss with passage of time.

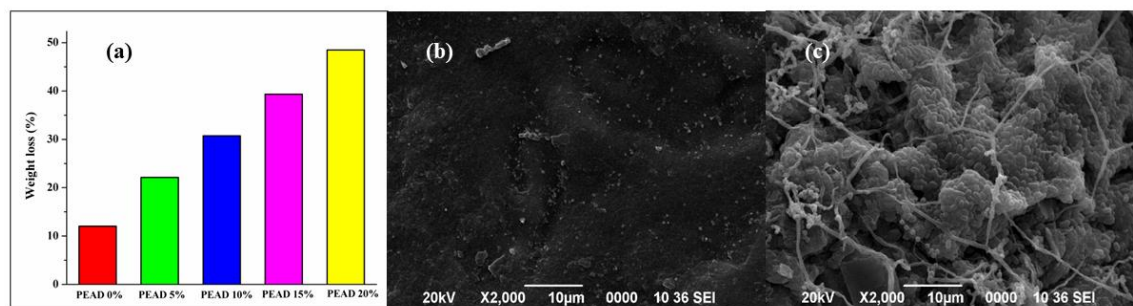


Figure 3.9. (a) Weight loss (%) profile; SEM images of PEAD 15% composition (b) control specimen and (c) biodegraded by soil microbes against exposure time.

The morphological study was carried out by conducting SEM analyses on the soil-exposed specimens. The figures as shown in **Figure 3.9.** (b) and (c) clearly depicted the differences between the virgin polymer and the polymer under exposure to soil microbes. The specimen under inspection showed immense roughness in comparison to the control sample which was found to possess a smooth texture without any traces of unevenness. This signified extensive surface erosion as well as the expanse of degradation carried out by the soil microorganisms on the polymer surface. All these results are found to be in correlation with the gravimetric weight loss profiles.

Thus, both the biodegradation assays as discussed above confirmed the biodegradability feature of the synthesized poly(ester amide urethane) material.

3.3.9 Cytotoxicity study

Cytotoxicity testing is considered as a crucial assay to perceive the toxic response of cells towards the samples taken under consideration. Herein, the cytotoxicity parameter was evaluated for poly(ester amide urethane) in both the solvents viz., DMSO and water against HEK 293 cells by undergoing MTT assay as well as morphology change study. It is a well-known fact that MTT assessment depends on reduction of MTT compound to purple formazan crystals by cells which are metabolically active in nature [35]. In turn, it is also a well-established matter that only those cells which are viable or metabolically active bear the potency to produce pyridine nucleotides which eventually carry out the reduction procedure and the end results are measured spectrophotometrically owing to the formation of intensely colored formazan. As per literature reports, activity exhibited by viable cells above 70% with reference to the control specimen viz., DMEM (cell activity: 100%)

suggest that they are highly compatible in nature as they refrain from releasing any toxic compounds [36]. In this study, it was found that all the poly(ester amide urethane) of different compositions in DMSO (all PEAD compositions) exhibited cell viability above 90% which inferred that these specimens are cytocompatible in nature as illustrated in **Figure 3.10 (a)**. The graph depicted in **Figure 3.10 (a)** enumerated the cell metabolic activity or cell viability (%) against various compositions of polymer extractions for an incubation period of 24 h as well as 48 h. On the other hand, it was observed that all poly(ester amide urethane) compositions in water displayed metabolic activity less than 70%. This highlighted the fact that these specimens are low toxic or less compatible to the

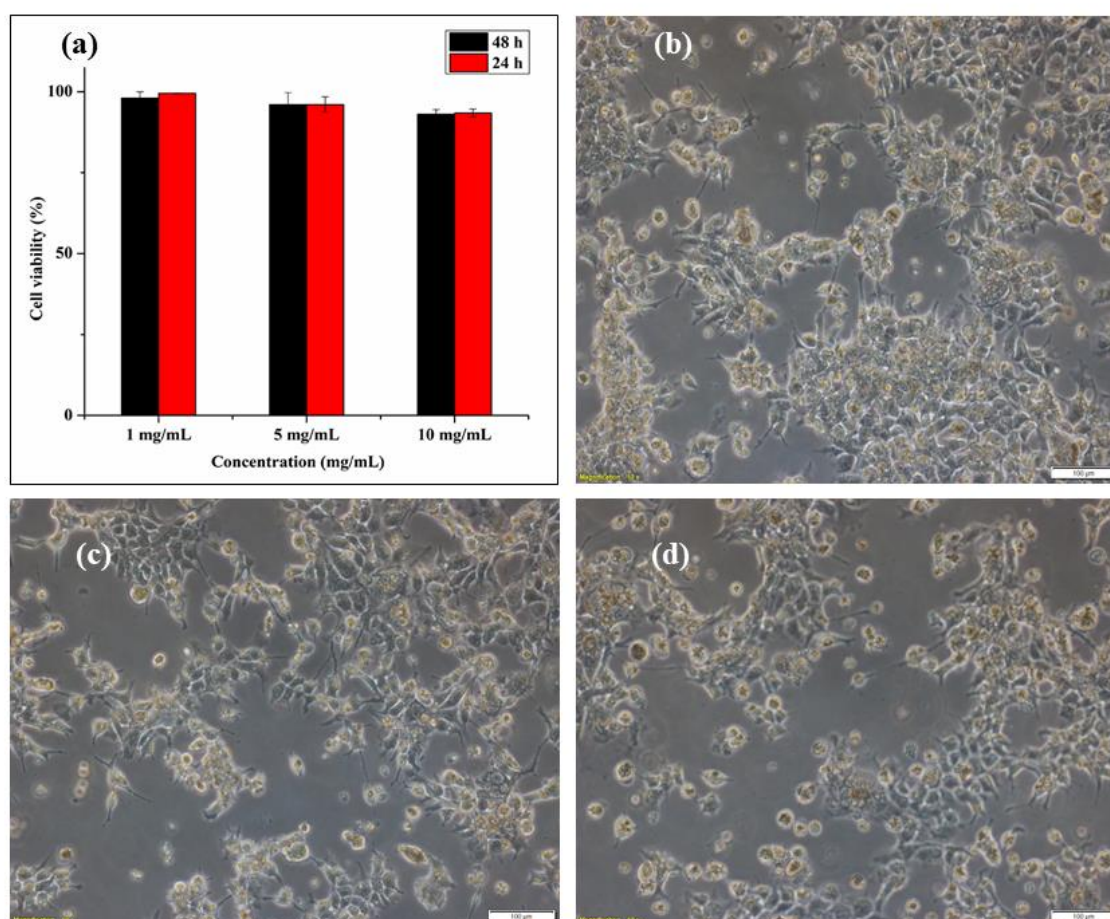


Figure 3.10 (a) *In-vitro* cytocompatibility test of PEAD 15% composition against concentration, and images of HEK-293 cells obtained using optical microscope **(b)** control specimen; after treatment with **(c)** 1 mg/mL concentration and **(d)** 5 mg/mL concentration of polymeric specimens against HEK-293 cells.

cells. The reason behind this result could be cited on the pretext of generation of amines in this system upon addition of water to the isocyanate unit, which are known to possess some toxicological properties and are considered lethal to the biological system.

In turn, the images of HEK-293 cells were obtained under an optical microscope as shown in **Figure 3.10 (b), (c) and (d)**. Comparative study between the control and treated specimens under varying concentrations highlighted the cytocompatibility trait of the polymeric material in an explicit manner.

3.4. Conclusion

From an all-inclusive study, it can be asserted that a tough, elastomeric, robust, biodegradable as well as biocompatible poly(ester amide urethane) material can be obtained using a simple, facile environmentally compatible route devoid of usage of any catalyst. In this present study, citric acid, hexamethylenediamine and glycerol were utilized as the core reactants followed by the use of IPDI as the primal substrate to improve the texture as well as upgrade the material performance test results. In turn, different instrumental analyses supported the formation of the polymeric material. Aging studies were also conducted in a comprehensive manner in order to explore the sturdiness of the material under various rigorous conditions. Moreover, the presence of biodegradability as well as biocompatibility attributes conferred new dimension to the material. Therefore, the existence of the above-mentioned features can ascribe its utility as a viable biodegradable and biocompatible material as well as a sustainable coating material.

References

- [1] Derksen, J. T., Cuperus, F. P., and Kolster, P. Paints and coatings from renewable resources. *Industrial Crops and Products*, 3(4):225-236, 1995.
- [2] Kenawy, E. R., Worley, S. D., and Broughton, R. The chemistry and applications of antimicrobial polymers: a state-of-the-art review. *Biomacromolecules*, 8(5):1359-1384, 2007.
- [3] Long, T. E. and Scheirs, J. editors. *Modern polyesters: chemistry and technology of polyesters and copolyesters*. John Wiley & Sons, 2005.

- [4] Vilela, C., Sousa, A. F., Fonseca, A. C., Serra, A. C., Coelho, J. F., Freire, C. S., and Silvestre, A. J. The quest for sustainable polyesters—insights into the future. *Polymer Chemistry*, 5(9):3119-3141, 2014.
- [5] Porta, R., Sabbah, M., and Di Pierro, P. Biopolymers as food packaging materials. *International Journal of Molecular Sciences*, 21(14):4942, 2020.
- [6] Zembyla, M., Murray, B. S., and Sarkar, A. Water-in-oil emulsions stabilized by surfactants, biopolymers and/or particles: A review. *Trends in Food Science & Technology*, 104:49-59, 2020.
- [7] Xiong, R., Grant, A. M., Ma, R., Zhang, S., and Tsukruk, V. V. Naturally-derived biopolymer nanocomposites: Interfacial design, properties and emerging applications. *Materials Science and Engineering: R: Reports*, 125:1-41, 2018.
- [8] Gandini, A. Polymers from renewable resources: a challenge for the future of macromolecular materials. *Macromolecules*, 41(24):9491-9504, 2008.
- [9] Winnacker, M. and Rieger, B. Poly (ester amide)s: recent insights into synthesis, stability and biomedical applications. *Polymer Chemistry*, 7(46):7039-7046, 2016.
- [10] Han, S. and Wu, J. Recent advances of poly (ester amide)s-based biomaterials. *Biomacromolecules*, 23(5):1892-1919, 2022.
- [11] Díaz, A., Katsarava, R., and Puiggali, J. Synthesis, properties and applications of biodegradable polymers derived from diols and dicarboxylic acids: from polyesters to poly (ester amide)s. *International Journal of Molecular Sciences*, 15(5):7064-7123, 2014.
- [12] Rodriguez-Galan, A., Franco, L., and Puiggali, J. Degradable poly (ester amide)s for biomedical applications. *Polymers*, 3(1):65-99, 2010.
- [13] Gogoi, G., Gogoi, S., and Karak, N. Dimer acid based waterborne hyperbranched poly (ester amide) thermoset as a sustainable coating material. *Progress in Organic Coatings*, 112:57-65, 2017.
- [14] Fonseca, A. C., Gil, M. H. and Simoes, P. N. Biodegradable poly (ester amide)s—A remarkable opportunity for the biomedical area: Review on the synthesis, characterization and applications. *Progress in Polymer Science*, 39(7):1291-1311, 2014.
- [15] Kadajji, V. G. and Betageri, G. V. Water soluble polymers for pharmaceutical applications. *Polymers*, 3(4):972-2009, 2011.
-

- [16] Froehling, P. Development of DSM's hybrane® hyperbranched poly(ester amide)s. *Journal of Polymer Science Part A: Polymer Chemistry*, 42(13):3110-3115, 2004.
- [17] Sharma, H. O., Alam, M., Riaz, U., Ahmad, S., and Ashraf, S. M. Miscibility studies of poly(ester amide)s of linseed oil and dehydrated castor oil with poly(vinyl alcohol). *International Journal of Polymeric Materials*, 56(4):437-451, 2007.
- [18] Dai, J., Ma, S., Liu, X., Han, L., Wu, Y., Dai, X., and Zhu, J. Synthesis of bio-based unsaturated polyester resins and their application in waterborne UV-curable coatings. *Progress in Organic Coatings*, 78:49-54, 2015.
- [19] Akindoyo, J. O., Beg, M., Ghazali, S., Islam, M. R., Jeyaratnam, N., and Yuvaraj, A. R. Polyurethane types, synthesis and applications—a review. *RSC Advances*, 6(115):114453-114482, 2016.
- [20] Varganici, C. D., Ursache, O., Gaina, C., Gaina, V. and Simionescu, B. C. Studies on new hybrid materials prepared by both Diels–Alder and Michael addition reactions. *Journal of Thermal Analysis and Calorimetry*, 111:1561-1570, 2013.
- [21] Macocinschi, D., Filip, D., Zaltariov, M. F., and Varganici, C. D. Thermal and hydrolytic stability of silver nanoparticle polyurethane biocomposites for medical applications. *Polymer Degradation and Stability*, 121:238-246, 2015.
- [22] Tang, B., Lin, X., Zou, F., Fan, Y., Li, D., Zhou, J., Chen, Wu., and Wang, X. In situ synthesis of gold nanoparticles on cotton fabric for multifunctional applications. *Cellulose*, 24:4547-4560, 2017.
- [23] Kar, A. and Karak, N. Bio-based poly (ester amide): mechanical, thermal and biodegradable behaviors. *Journal of Polymer Research*, 29(9):366, 2022.
- [24] Gogoi, G. and Karak, N. Waterborne hyperbranched poly (ester amide urethane) thermoset: Mechanical, thermal and biodegradation behaviors. *Polymer Degradation and Stability*, 143:155-163, 2017.
- [25] Zhang, R., Yu, S., Shi, W., Wang, W., Wang, X., Zhang, Z., Li, L., Zhang, B., and Bao, X. A novel poly(ester amide) thin film composite nanofiltration membrane prepared by interfacial polymerization of serinol and trimesoyl chloride (TMC) catalyzed by 4-dimethylaminopyridine (DMAP). *Journal of Membrane Science*, 542:68-80, 2017.
-

- [26] El-Shamy, A. G., Attia, W., and Abd El-Kader, K. M. The optical and mechanical properties of PVA-Ag nanocomposite films. *Journal of Alloys and Compounds*, 590:309-312, 2014.
- [27] Fong, R. J., Robertson, A., Mallon, P. E., and Thompson, R. L. The impact of plasticizer and degree of hydrolysis on free volume of poly (vinyl alcohol) films. *Polymers*, 10(9):1036, 2018.
- [28] Nielsen, L. E. Cross-linking—effect on physical properties of polymers. *Journal of Macromolecular Science, Part C*, 3(1):69-103, 1969.
- [29] Weon, J. I. Effects of thermal ageing on mechanical and thermal behaviors of linear low density polyethylene pipe. *Polymer Degradation and Stability*, 95(1):14-20, 2010.
- [30] Wang, Q. W., Yoon, K. H., and Min, B. G. Chemical and physical modification of poly (p-phenylene benzobisoxazole) polymers for improving properties of the PBO fibers. I. Ultraviolet-ageing resistance of PBO fibers with naphthalene moiety in polymer chain. *Fibers and Polymers*, 16:1-7, 2015.
- [31] Vahabi, H., Sonnier, R., and Ferry, L. Effects of ageing on the fire behaviour of flame-retarded polymers: a review. *Polymer International*, 64(3):313-328, 2015.
- [32] Pramanik, S., Konwarh, R., Sagar, K., Konwar, B. K., and Karak, N. Biodegradable vegetable oil based hyperbranched poly (ester amide) as an advanced surface coating material. *Progress in Organic Coatings*, 76(4):689-697, 2013.
- [33] Rudnik, E. and Briassoulis, D. Comparative biodegradation in soil behaviour of two biodegradable polymers based on renewable resources. *Journal of Polymers and The Environment*, 19:18-39, 2011.
- [34] Chin, K. M., Sam, S. T., Ong, H. L., Wong, Y. S., and Tan, W. K. Biodegradation improvement of bioinspired crosslinked and noncrosslinked polyvinyl alcohol nanocomposites with cellulose nanocrystals extracted from rice straw through natural soil burial exposure. *Polymer Composites*, 43(10):6955-6965, 2022.
- [35] Xu, L. and Yamamoto, A. Characteristics and cytocompatibility of biodegradable polymer film on magnesium by spin coating. *Colloids and Surfaces B: Biointerfaces*, 93:67-74, 2012.
- [36] Gupta, K., Barua, S., Hazarika, S. N., Manhar, A. K., Nath, D., Karak, N., Namsa, N. D., Mukhopadhyay, R., Kalia, V. C., and Mandal, M. Green silver
-

nanoparticles: enhanced antimicrobial and antibiofilm activity with effects on DNA replication and cell cytotoxicity. *RSC Advances*, 4(95):52845-52855, 2014.